

## ARTICLE

# Theoretical Studies on Electronic Structures and Spectroscopy of Fluorescent Arylamino Fumaronitrile

Xiao-peng Chen, Yu-qi Ding, Qi-wen Teng\*

*Department of Chemistry, Zhejiang University, Hangzhou 310027, China*

(Dated: Received on May 3, 2007; Accepted on June 4, 2007)

A new series of fluorescent arylamino fumarinitrile derivatives was designed and optimized using density function theory at the B3LYP/6-31G\* level. Based on the optimized geometries, the electronic, fluorescent and  $^{13}\text{C}$  NMR spectra are calculated with INDO/CIS, CIS-ZINDO TD, and B3LYP/6-31G\* methods, respectively. Starting with the first of the series, the LUMO-HOMO energy gaps of the derivatives become wider and the fluorescent wavelengths and the main peaks in the electronic spectra are blue-shifted owing to the large steric effect of naphthyl rings. On the contrary, the energy gaps of the derivatives turn narrow, and the fluorescent wavelengths and the main peaks in the electronic spectra are red-shifted since hydroxyl groups improve the symmetry and extend the conjugation system. The chemical shifts of  $\text{sp}^2\text{-C}$  on the phenyl rings are moved upfield, while chemical shifts of carbon atoms on the cyano groups and those connected with the cyano groups are changed downfield in the presence of hydroxyl groups.

**Key words:** Arylamino fumaronitrile, Fluorescence, Energy gap, B3LYP/6-31G\*

## I. INTRODUCTION

Organic light-emitting diodes (OLEDs) have entered the electronic market, which has been dominated by the liquid-crystal display (LCD) for the past several years [1-9]. Lee *et al.* has synthesized triphenylamine as a hole-injecting and transporting layer in the light-emitting material, and enhanced the efficiency of the device [1]. Chen *et al.* has achieved blue light-emitting compounds containing anthracene, naphthalene and fluorene units. Their higher hole-mobility leads to the longer lifetime and lower drive voltage of the device [2]. Monomethyl maleate copolymers with triarylamine are employed to fabricate anode-interface layers that can promote the interfacial cohesion in OLEDs [3]. Several side-chain polymers functionalized with hole-transporting units are characterized, which can be used to prepare solution-based multilayer OLEDs [4]. Besides this, single-walled carbon nanotube (SWNT) films can be transferred on the polyethyleneterephthalate substrates. These materials act as the anodes in OLEDs, and exhibit many advantages in the aspects of nanoporous structure, moderate preparation, excellent acid resistance, and mechanical flexibility [5]. An efficient green electrophosphorescent material has been obtained by linking carbazole and fluorene moieties as well [6]. A novel arylamino fumaronitrile derivative has been accomplished, which is utilized as a red OLED material [7]. It is weakly emissive in solution but highly fluorescent in the solid state. Its photophysical properties are worth further exploration. Optical, electrochemical

and thermal properties of other non-doping arylamino fluorescent materials are widely studied [8-10].

However, there are few theoretical studies on electronic structures and spectroscopy of arylamino fumarinitrile. Thus a series of fluorescent arylamino fumarinitrile molecules are designed. Their characters such as HOMO-LUMO energy gap, ionization potential, electron affinity, absolute hardness, absolute electron negativity, luminescent wavelength, and other spectra are explored.

## II. THEORETICAL METHODS

Small molecules often have wide band gaps. The extension of the conjugation system is beneficial to reduce the energy gap of the molecule. The molecules with the small energy gaps become red fluorescent materials. But the extended conjugation system decreases the solubility of the compounds. Thus substituents on side chains are utilized to increase the solubility. Based on the above consideration, a series of aryl rings and hydroxyl groups are introduced into the studied molecules. The arylamino fumarinitrile derivatives (compounds 1-8) were designed by changing substituents of aryl and hydroxyl groups, whereas compound 9 was formed by replacing the nitrogen atoms in compound 2 using the carbon and hydrogen atoms (Fig.1). Full geometry optimization without any symmetry restrictions for these compounds was performed using AM1 and the B3LYP/STO-3G, B3LYP/3-21G and B3LYP/6-31G\* methods in the GAUSSIAN 03 program, step by step [11]. These methods are often used to study the energies and structures of supramolecular complexes [12-14] and conducting polymers [15,16] as well as other organic compounds [17,18]. Then the equilibrium geometries

\* Author to whom correspondence should be addressed. E-mail: wushi@zju.edu.cn

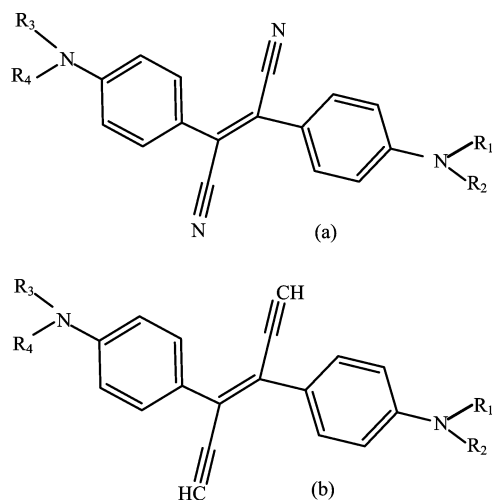


FIG. 1 The structural schemes of (a) compounds 1-8 and (b) compound 9. Compound 1:  $R_1=R_2=R_3=R_4$ =phenyl; Compound 2:  $R_1=R_3$ =phenyl,  $R_2=R_4$ = $\alpha$ -naphthyl; Compound 3:  $R_1=R_2=R_3=R_4$ = $\alpha$ -naphthyl; Compound 4:  $R_1=R_2=R_3$ =phenyl,  $R_4$ =*p*-hydroxylphenyl; Compound 5:  $R_1=R_3$ =phenyl,  $R_2=R_4$ =*p*-hydroxylphenyl; Compound 6:  $R_1=R_2$ =phenyl,  $R_3=R_4$ =*p*-hydroxylphenyl; Compound 7:  $R_1=R_4$ =phenyl,  $R_2=R_3$ =*p*-hydroxylphenyl; Compound 8:  $R_1=R_2=R_3=R_4$ =*p*-hydroxylphenyl; Compound 9:  $R_1=R_3$ =phenyl,  $R_2=R_4$ = $\alpha$ -naphthyl.

were determined.

According to Koopman's theory, vertical ionization potential ( $IP_v$ ) is approximately defined as the negative value of HOMO (the highest occupied molecular orbitals) energy, whereas vertical electron affinity ( $EA_v$ ) is approximately defined as the negative value of LUMO (the lowest unoccupied molecular orbitals) energy. Absolute hardness ( $\eta$ ) is equal to the half of the difference between  $IP_v$  and  $EA_v$ , while absolute electron negativity ( $\chi$ ) is defined as the half of the sum for  $IP_v$  and  $EA_v$ . All these values are calculated at the B3LYP/6-31G\* level.

In spite of the better precision of time-dependent density functional theory (TD-DFT) compared to the semiempirical method, there is still a more serious defect in accuracy when comparing TD-DFT calculated results with experimental ones [15]. Therefore the INDO/CIS method without any adjustment of parameters [19-28] is used here to investigate the configuration interaction on the basis of the B3LYP/6-31G\* optimized geometries of compounds 1-9. One hundred and ninety-seven configurations including the ground state are states generated by exciting electrons from the 14 HOMO into the 14 LUMO. Then the wavelength  $\lambda$  and oscillator strength  $f$  were obtained. Fluorescent wavelengths were calculated with the CIS-ZINDO TD method. The chemical shifts in  $^{13}\text{C}$  NMR spectra of the compounds were calculated with the GIAO method at B3LYP/6-31G level.

### III. RESULTS AND DISCUSSION

#### A. HOMO-LUMO energy gap

There is a strong dependence of fluorescent wavelength for the derivative on the LUMO-HOMO energy gap. The energy gaps of compounds 1-8 are all around 2.6 eV except the 3.1 eV of compound 9 (Table I). Those of compounds 1-3 gradually increase. The conjugation system becomes less with the substitution of more aryl groups. This is caused by the large steric effect of the bulky naphthyl groups. Actually, there exist easily exchangeable multiple conformations of nonplanar phenyl and naphthyl rings [7]. The energy gaps of compounds 1, 4, 5, and 8 successively decrease. The presence of more and more hydroxyl groups on the phenyl rings leads to the extended conjugation system, which reduces the energy gap. In addition, the energy gap is further lessened when the two hydroxyl groups are located at the neighboring phenyl rings on the same nitrogen atom, thus compound 6 has a lower energy gap than compound 5. In contrast, the energy gap of compound 7 compared to that of compound 5 becomes large since the two hydroxyl groups are separated far away from each other. The energy gap of compound 9 is larger than that of compound 2. The carbon atoms in compound 9 compared to the nitrogen atoms in compound 2 have less electronegativity, which results in greater electron density on the backbone and elevation of the LUMO energy (see Table I).

TABLE I Some variables of compounds 1-9 at B3LYP/6-31G\* level

Compound	Energy gap/eV	$IP_v$ /eV	$EA_v$ /eV	$\eta$ /eV	$\chi$ /eV
1	2.609	5.052	2.443	1.305	3.747
2	2.655	5.063	2.409	1.327	3.736
3	2.696	5.060	2.364	1.348	3.712
4	2.583	4.977	2.394	1.292	3.686
5	2.554	4.921	2.367	1.277	3.644
6	2.538	4.905	2.368	1.269	3.637
7	2.562	4.924	2.363	1.281	3.642
8	2.507	4.787	2.280	1.254	3.533
9	3.102	4.777	1.675	1.551	3.226

#### B. Some important variables

According to the electrofluorescent mechanism based on the theory of semiconductors, the chemical fluorescence is produced by the radiative transition of electrons in an excited molecule. The holes and electrons are injected on the anode and cathode respectively under the existence of the external electrical field. They are transported in the transporting layer as hopping partners, and then approach the emitting layer. When

they meet, the excited molecule is formed. Molecules of the smaller  $IP_v$  make it easy to inject the holes, whereas molecules of the higher  $EA_v$  make it easy to inject the electrons. The  $IP_v$  values of compounds 2 and 3 are bigger than that of compound 1 (Table I). The electrons in HOMO of compounds 2 and 3 are distributed to the naphthyl rings, and are not easily lost. The  $IP$  values of compounds 1, 4, 5, and 8 gradually decrease, which indicates that the electrons in HOMO of 1, 4, 5, and 8 are easily lost and the holes are easily injected progressively. This phenomenon is caused by the electron-donating effect of the growing number of hydroxyl groups in compounds 1, 4, 5, and 8. The  $IP_v$  value of compound 6 is less, whereas the  $IP_v$  value of compound 7 is bigger than that of compound 5. The approach of the two hydroxyl groups in compound 6 leads to the more obvious electron-donating effect. The  $IP_v$  datum of compound 9 is less than that of compound 2 because the carbon atoms in compound 9 possess bad electronegativity and easily lose electrons, compared to the nitrogen atoms in compound 2.

The  $EA_v$  data in order of compounds 1, 2, and 3 have decrease, so do those of compounds 1, 4, 5, and 8. Compounds do not easily gain electrons when the naphthyl rings are introduced or the number of the hydroxyl groups is increased, individually. The  $EA_v$  value of compound 6 is greater, whereas the  $EA_v$  value of compound 7 is less than that of compound 5. The nearer the two hydroxyl groups are, the easier the electrons are injected. Compound 9 has the least electron affinity because it has no cyano groups. The changing trend of  $\chi$  almost exhibits the similar conclusion drawn from that of  $IP$ . The  $\chi$  values of compounds 1, 4, 5, and 8 are successively reduced, which show the lower oxidation-resisting abilities of these compounds. The electrons in HOMO of these compounds are easily lost. There is a little difference among the  $\chi$  data of compounds 5, 6, and 7. The  $\chi$  value of compound 9 is the least, thus it is ready to lose electrons in HOMO and accept the positive charges.

The  $\eta$  values of compounds 2 and 3 are higher than that of compound 1, thus compounds 2 and 3 possess higher stabilities. The more naphthyl rings in compounds 2 and 3 can better contain electrons, and then the thermal stabilities are improved. The  $\eta$  values of compounds 1, 4, 5, and 8 are decreased in turn, and these compounds are less and less stable. The electron-donating effect of the more hydroxyl groups is unfavorable to disperse electrons, which reduces thermal stabilities of the above compounds. Compound 6 owns the least  $\eta$  value, while compound 7 displays a larger  $\eta$  value than that of compound 5. The energy gap of compound 6 is less. At the same time, the oxidative and reductive characters of compound 6 are obvious. Therefore, compound 6 is reactive and possesses less thermal stability. Compound 9 has bigger absolute hardness, thus is more thermally stable than the others studied. Obviously, the presence of the heteroatoms in compounds 1-8 reduces

their stabilities.

### C. Electronic absorption spectra

The main absorption peaks in the electronic spectrum of compound 1 appear at 345.4, 279.1, and 190.8 nm (Fig.2). The first absorption at 342.6 nm of compound 2 which is symmetry-allowed mainly arises from the electronic transition of HOMO (122) to LUMO (123) regarding the valence electrons of INDO method. It is blue-shifted, compared to that of compound 1, which is caused by the elevation of the LUMO-HOMO energy gap of compound 2. The main absorption at 214.9 nm of compound 2 is red-shifted, compared to 190.8 nm of compound 1. This absorption arises from occupied orbital (120) to the virtual (127). The molecular orbitals (127) and (120) are basically composed of the atomic orbitals  $p_x$  of the bridged carbon atoms and the carbon atoms connecting to the nitrogen atoms on the naphthyl rings according to the coefficients of the molecular orbitals. These carbon atoms are located on the naphthyl rings. Therefore the red-shift of this absorption is relevant to the change in electron cloud on the naphthyl rings.

The main absorptions at 196.2 and 284.1 nm of compound 4 and at 196.4 and 287.1 nm of compound 6 are red-shifted relative to those of compound 1. This arises from the narrow energy gaps of compounds 4 and 6 when the hydroxyl groups exist. The appearances of the electronic spectra of compounds 5 and 6 are analogous as the number of the hydroxyl groups in the two compounds is the same. There is still a little red-shift in the main absorptions at 196.4, 287.1, and 393.6 nm of compound 6 relative to 193.9, 284.8, and 393.0 nm of compound 5, which is caused by the lower energy gap and easier donation of electrons when the two hydroxyl groups in compound 6 are close. Furthermore, the first peaks of compounds 1, 4, 6, and 8 are red-shifted in turn as the number of the hydroxyl groups is elevated step by step.

The first peak at 322.4 nm of compound 9, chiefly caused by the electronic transition from HOMO (122) to LUMO (123), is blue-shifted compared with that of compound 2. The HOMO (122) and LUMO (123) of compound 9 are mainly composed of  $p_y$  orbitals of the two carbon atoms used to substitute nitrogen atoms in compound 2, and the absolute values of combination coefficients are 0.1286 and 0.2280. Thereby these two carbon atoms participate in the formation of HOMO (122) and LUMO (123) in compound 9. The energy gap of compound 9 is wider than that of compound 2. The main peaks at 282.9 and 305.5 nm of compound 9 relative to 294.7 and 307.6 nm of compound 2 are also blue-shifted. There is an obvious impact of acetylene groups in compound 9 on the absorptions in the electronic spectrum.

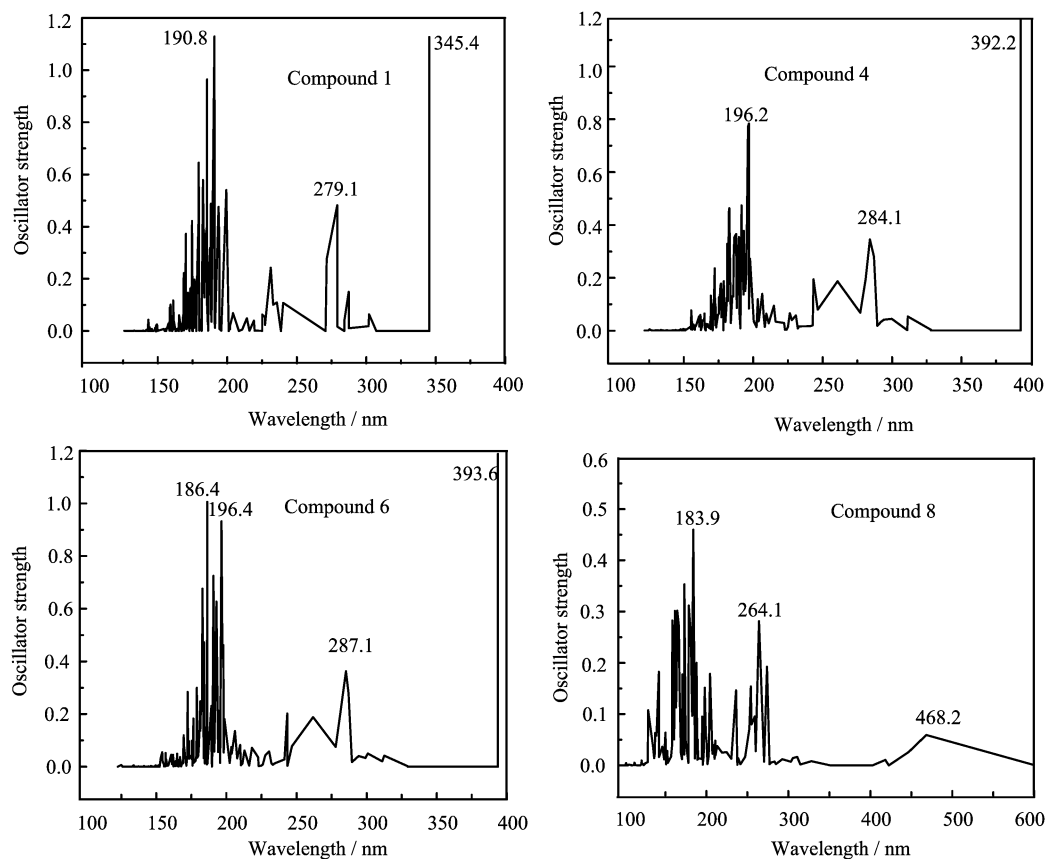


FIG. 2 Electronic spectra of compounds 1, 4, 6, and 8 using INDO/CIS method.

#### D. Fluorescent spectra

The fluorescent wavelengths and oscillator strength are two important characteristics measuring the properties of fluorescent materials. These two variables can be determined experimentally and computed theoretically. The fluorescent wavelengths of compounds 1-8 (Table II) are around 420 nm except 390 nm of compound 9, and oscillator strength of these absorptions is strong. Then these compounds can be easily excited at the wavelength of 420 nm. The wavelengths of compounds 2 and 3 in comparison with that of compound 1 are a little blue-shifted. The steric effect of the  $\alpha$ -naphthyl groups blocks the extension of the conjugation system, which enhances the energy gaps of compounds 2 and 3. The wavelengths of compounds 1, 4, 5, and 8 are red-shifted gradually. The presence of the more hydroxyl groups benefits the coplanar arrangement of the naphthyl rings and enlarges the conjugation system. This impact decreases the energy gaps of the compounds, and electrons are easy to excite. The fluorescent wavelength of compound 6 is red-shifted, whereas the fluorescent wavelength of compound 7 is blue-shifted, relative to that of compound 5. These results also correspond to their energy gaps. Analogously, compound 9 without the cyano group has the shortest excited wave-

length, which is related to its wider energy gap. The experiment shows that compound 2 can be prepared by vacuum deposition and excited by using 420 nm as excitation energy [7]. The calculated fluorescent wavelength of compound 2 is 418.7 nm, which is in agreement with the experiment. Then the fluorescent wavelengths predicted theoretically of the other compounds shown in Table II are reliable.

TABLE II Fluorescent wavelengths of compounds 1-9 using CIS-ZINDO TD method

Compound	$\lambda$ /nm	$f$	Compound	$\lambda$ /nm	$f$
1	419.6	1.0613	6	422.0	1.0760
2	418.7	1.1310	7	420.2	1.0695
3	419.5	1.1148	8	423.2	1.0899
4	420.3	1.0693	9	390.3	0.9586
5	421.2	1.0775			

#### E. NMR spectra

The change in electron density of carbon atoms can be reflected by chemical shifts in the  $^{13}\text{C}$  NMR spectrum, which is helpful to explore the effect of sub-

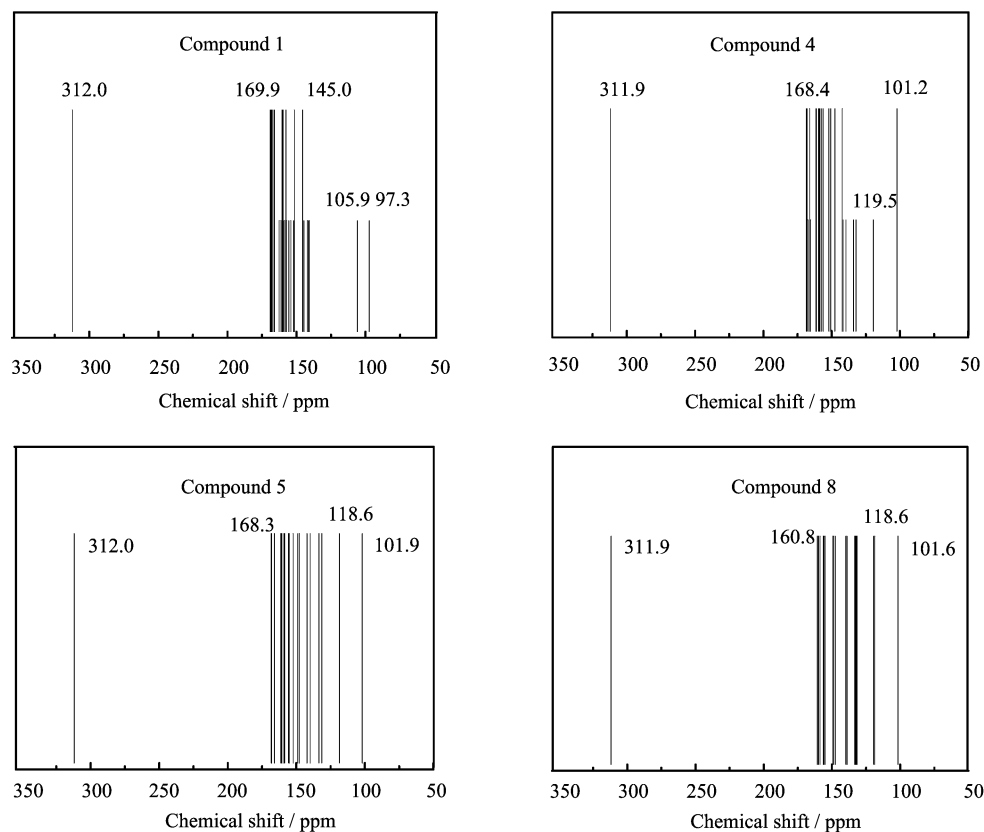


FIG. 3  $^{13}\text{C}$  NMR spectra of compounds 1, 4, 5, and 8 at B3LYP/6-31G level.

stituents. The chemical shifts around 100 ppm and at 312.0 ppm in the  $^{13}\text{C}$  NMR spectrum of compound 1 are attributed to  $\text{sp}^2\text{-C}$  on the cyano groups and  $\text{sp}^2\text{-C}$  connected with the cyano groups, respectively. While the chemical shifts at 145.0-169.9 ppm are assigned as  $\text{sp}^2\text{-C}$  on benzene rings (Fig.3). Compound 1 is  $\text{C}_{2v}$  symmetrical, thus the intensity of the absorptions is 2. However, some peaks are split, and the intensity becomes 1. The steric effect of phenyl groups destroys the symmetry, and thus the number of absorptions is increased.

The chemical shifts of  $\text{sp}^2\text{-C}$  in compound 4 compared with those of compound 1 are changed upfield from 140.6 ppm to 119.5 ppm. The electron density on the carbon atoms is increased and the shielding effect improved when the hydroxyl group is present. The peak at 101.2 ppm in compound 4 corresponds to the two peaks at 105.9 and 97.3 ppm in compound 1. Therefore, the symmetry of compound 4 is improved due to the presence of the hydroxyl groups.

In comparison with the chemical shifts of  $\text{sp}^2\text{-C}$  in compound 4, those in compound 5 are moved upfield within the range of 168.3-118.6 ppm, which is ascribed to the contribution of the two hydroxyl groups on the phenyl rings. While those on the cyano groups and those connected with the cyano groups in compound 5 are changed downfield. There is a little difference

in chemical shifts between compound 5 and compound 6. In compound 7, the chemical shifts of  $\text{sp}^2\text{-C}$  remain unchanged, and those on the cyano groups and those connected with the cyano groups are transferred upfield. Generally, subtle differences are produced when the sites of hydroxyl groups are changed. The number of the absorptions in the NMR spectra of compounds 5 and 8 relative to those of compound 1 is reduced relative to those of compounds 1 and 4. The presence of more hydroxyl groups in compounds 5 and 8 inhibits the geometry rotation of the aryl groups, and the molecular symmetry is ameliorated. Moreover, the presence of the four hydroxyl groups in compound 8 elevates the electron density on the aryl rings, thus the chemical shifts of  $\text{sp}^2\text{-C}$  are turned into the upfield area within 160.8-118.6 ppm, relative to 168.4-119.5 ppm in compound 4.

#### IV. CONCLUSION

The electronic structure and spectral characters of the arylamino fumaronitrile are affected by aryl rings, hydroxyl groups, and cyano groups on the skeleton. The aryl rings are favorable to distribute electrons and improve the thermal stabilities. But the conformations are twisted, and the energy gaps are increased thanks

to the large steric effect of the aryl groups. The energy gaps of the derivatives are reduced and the fluorescent wavelengths are red-shifted in the presence of the hydroxyl groups on the aryl rings. Furthermore, the energy gap is reduced when the two hydroxyl groups are located at the neighboring phenyl rings on the same nitrogen atom. Besides, the molecular symmetry can be improved, and the solubility enhanced as the hydroxyl groups are increased. Heteroatoms on the backbone are also advantageous to decrease the energy gap. The presence of hydroxyl groups benefits the injection of holes, while the presence of cyano groups favors the injection of electrons. Thus, this kind of fluorescent material should be comprehensively designed based on the above factors so that the holes and electrons are both easy to inject and transport at almost the same speed in the solid state. Only in this way can the holes and electrons reach the emitting layer simultaneously. Then an excellent electroluminescent material can be made.

- [1] J. Li, C. Ma, J. Tang, C. S. Lee, and S. Lee, *Chem. Mater.* **17**, 615 (2005).
- [2] S. W. Culligan, A. C. A. Chen, J. U. Wallace, K. P. Klubek, C. W. Tang, and S. H. Chen, *Adv. Funct. Mater.* **16**, 1481 (2006).
- [3] S. Kato, *J. Am. Chem. Soc.* **127**, 11538 (2005).
- [4] E. Bacher, M. Bayerl, P. Rudati, N. Reckefuss, C. D. Muller, K. Meerholz, and O. Nuyken, *Macromolecules* **38**, 1640 (2005).
- [5] J. Li, L. Hu, L. Wang, Y. Zhou, G. Gruner, and T. J. Marks, *Nano. Lett.* **6**, 2472 (2006).
- [6] K. T. Wong, Y. M. Chen, Y. T. Lin, H. C. Su, and C. C. Wu, *Org. Lett.* **7**, 5361 (2005).
- [7] H.C. Yeh, S. J. Yeh, and C. T. Chen, *Chem. Commun.* 2632 (2003).
- [8] W. C. Wu, H.C. Yeh, L. H. Chan, and C. T. Chen, *Adv. Mater.* **14**, 1072 (2002).
- [9] Q. Huang, J. Li, G. A. Evmenenko, P. Dutta, and T. J. Marks, *Chem. Mater.* **18**, 2431 (2006).
- [10] Z. H. Li and M. S. Wong, *Org. Lett.* **8**, 1499 (2006).
- [11] M. J. Frisch, G. W. Trucks, H. B. Schlegel, G. E. Scuseria, M. A. Robb, J. R. Cheeseman, V. G. Zakrzewski, J. A. Montgomery, R. E. Stratmann, J. C. Burant, S. Dapprich, J. M. Millam, A. D. Daniels, K. N. Kudin, M. C. Strain, O. Farkas, J. Tomasi, V. Barone, M. Cossi, R. Cammi, B. Mennucci, C. Pomelli, C. Adamo, S. Clifford, J. Ochterski, G. A. Petersson, P. Y. Ayala, Q. Cui, K. Morokuma, D. K. Malick, A. D. Rabuck, K. Raghavachari, J. B. Foresman, J. Cioslowski, J. V. Ortiz, B. B. Stefanov, G. Liu, A. Liashenko, P. Piskorz, I. Komaromi, R. Gomperts, R. L. Martin, D. J. Fox, T. Keith, M. A. Al-Laham, C. Y. Peng, A. Nanayakkara, C. Gonzalez, M. Challacombe, P. M. W. Gill, B. G. Johnson, W. Chen, M. W. Wong, J. L. Andres, M. Head-Gordon, E. S. Replogle, and J. A. Pople, *Gaussian 03, Revision B 01*, Pittsburgh, PA: Gaussian Inc, (2003).
- [12] S. Wu and Q. W. Teng, *Chin. J. Chem. Phys.* **19**, 76 (2006).
- [13] Z. F. Wang and S. Wu, *Chem. Pap.*, **61**, 313 (2007).
- [14] C. Yan, N. H. Su, and S. Wu, *Russ. J. Phys. Chem.* **81**, 1980 (2007).
- [15] L. Yang, A. M. Ren, J. K. Feng, and J. F. Wang, *J. Org. Chem.* **70**, 3009 (2005).
- [16] M. H. Xie, N. H. Su, and S. Wu, *Chin. J. Struct. Chem.* (2007) in press.
- [17] H. Song, X. Y. Wang, and X. M. Yang, *Chin. J. Chem. Phys.* **19**, 281 (2006).
- [18] H. Y. Yu, B. Z. Li and Y. M. Guo, *Chin. J. Chem. Phys.* **19**, 233 (2006).
- [19] M. A. Thompson and M. C. Zerner, *J. Am. Chem. Soc.* **113**, 8210 (1991).
- [20] X. F. Xu, Y. M. Xing, X. Yang, G. C. Wang, Z. S. Cai, Z. F. Shang, Y. M. Pan, and X. Z. Zhao, *Int. J. Quantum Chem.* **101**, 160 (2005).
- [21] S. Wu and Q. W. Teng, *Chin. J. Chem. Phys.* **19**, 301 (2006).
- [22] S. Wu and Q. W. Teng, *Chin. J. Chem. Phys.* **18**, 715 (2005).
- [23] Q. W. Teng and S. Wu, *J. Mol. Struct. (THEOCHEM)* **756**, 103 (2005).
- [24] S. Wu and Q. W. Teng, *Int. J. Quantum Chem.* **106**, 526 (2006).
- [25] Q. W. Teng and S. Wu, *Chin. J. Chem. Phys.* **18**, 559 (2005).
- [26] Q. W. Teng, S. Wu, and M. Xie, *Chin. J. Chem. Phys.* **19**, 223 (2006).
- [27] S. Wu, Q. W. Teng, and S. C. Chen, *Chin. J. Chem. Phys.* **20**, 155 (2007).
- [28] Y. Zhu, Q. Yin, L. Cao, Y. Yang, Y. Kan, and Z. Su, *Chin. J. Chem. Phys.* **17**, 126 (2004).